Anisotropic reorientational relaxation of biphenyl: Transient grating optical Kerr effect measurements

F. W. Deeg,[a] John J. Stankus, S. R. Greenfield, Vincent J. Newell, and M. D. Fayer
Department of Chemistry, Stanford University, Stanford, California 94305

(Received 1 February 1989; accepted 6 March 1989)

Subpicosecond transient grating optical Kerr effect measurements have been used to evaluate the reorientation of biphenyl molecules in neat biphenyl and *n*-heptane solutions. Besides an ultrafast (100 fs time scale) component associated with librational damping/dephasing, two reorientational relaxation components are observed. The slow reorientation is due to rotation around the short axes of the molecule (tumbling motion), the fast reorientation is associated with internal rotation around the central C–C bond and/or rotation of the whole molecule around its long axis (spinning motion). Whereas the tumbling motion has been observed in earlier depolarized light scattering data, the time resolved Kerr data presented here are the first ones to reveal the dynamics of the fast reorientation component and the ultrafast librational dynamics. It is shown that the diffusive reorientational relaxation must be coupled to the ultrafast librational dynamics, and implications of this coupling are pointed out.

I. INTRODUCTION

A large variety of spectroscopic methods, e.g., neutron scattering, nuclear magnetic resonance (NMR) and electron spin resonance (ESR) line shape analysis, Raman scattering, infrared absorption, fluorescence depolarization, dynamic light scatering (DLS), and optical Kerr effect (OKE), have been used to investigate the dynamics of molecules in liquids. Each experiment probes a different dynamical quantity and in general a different time correlation function.[1–3] Therefore, each approach can focus on a different aspect of the dynamics and contribute to a more detailed picture of the molecular motions. Even if two experimental setups measure the same dynamic variable and theoretically contain the same information, one of the two approaches may be advantageous due to experimental constraints like signal/noise (S/N) ratio or resolution and range of the measured parameters.

DLS experiments have been an extremely valuable tool in the investigation of rotational relaxation dynamics. Depending on the chosen optical technique (grating or interferometer filter, optical mixing) DLS can cover time scales from subpicoseconds to seconds and, therefore, measure reorientational motion of small molecules as well as macromolecules.[1] With the development of picosecond spectroscopy, direct measurements of orientational correlation functions became feasible, and there have been time resolved studies of the rotational relaxation of medium sized molecules with rotational diffusion constants in the 100 ps range using fluorescence depolarization or other polarization spectroscopic methods.[4] On the other hand, time domain measurements of the rotational dynamics of *small* molecules have been very scarce and there exist only a few OKE studies in this field since the advent of femtosecond laser pulses.[5–11] These studies served either as a pure demonstration of the effect or focused solely on the ultrafast dynamics ($0 < \tau < 500$ fs) associated with inertial motion of the molecules, dephasing/thermalization of the molecular libration and other interaction or collision induced effects.

In this paper we present a transient grating OKE study of the rotational dynamics of the biphenyl molecule in neat biphenyl and in *n*-heptane solutions based on a sub-ps time resolved transient grating (TG) approach. A TG approach to study the OKE was first used by Eyring and Fayer.[12] Preliminary data in a recently published DLS study of biphenyl/*n*-heptane solutions[13] have been interpreted with a single Lorentzian associated with the (comparatively slow) tumbling motion of the biphenyl molecule. We will compare the results of our time domain experiment with that frequency study focusing especially on the anisotropy of the molecular reorientation. We will also discuss the relationship between the ultrafast coherent librational motion of the molecules and the "incoherent" orientational dynamics due to diffusive reorientational relaxation on a slower time scale.

II. EXPERIMENTAL PROCEDURES

The laser system used has been described in detail elsewhere.[14] The 70 ps output pulses of a cw mode-locked Nd:YAG laser at a repetition rate of 83 MHz are sent through an optical pulse compressor and frequency doubled. The resulting 2.5 ps pulses at 532 nm with an average power of 750–800 mW are used to synchronously pump a linear astigmatically compensated three mirror dye laser which is tuned by a single plate birefringent filter. With DCM the dye laser delivers tunable 300 fs pulses with an average output of 70–220 mW over the wavelength range 605–705 nm. These dye pulses are amplified by pumping a three stage amplifier with frequency doubled pulses from a cavity-dumped, *Q*-switched, and mode-locked Nd:YAG laser operating at 1 kHz repetition rate. The cavity-dumped Nd:YAG laser produces 1 mJ IR pulses which, when frequency doubled, generate 700 μJ pulses at 532 nm to pump the three amplifier stages. The two Nd:YAG lasers are electronically synchronized by a common radio frequency (rf) master oscillator for both mode lockers and the timing is set by a voltage controlled phase shifter for the rf into the amplifying laser's

[a] Permanent address: Institut für Physikalische Chemie, Universität München, Sophienstrasse 11, 8000 München 2, Federal Republic of Germany.

 0021-9606/89/126893-10$02.10

mode locker. A saturable absorber jet between the second and third amplifier stage suppresses the unamplified dye pulses and shortens the width of the amplified pulse. For DCM we find typically pulsewidths of ~200 fs with an average pulse energy of 10–20 μJ. A laser wavelength of 665 nm was chosen to eliminate two-photon absorption in these experiments and similar experiments on pentylcyanobiphenyl which will be described in future publications.[15] To eliminate amplitude fluctuations of the amplified pulses due to timing jitter between the amplifying pulses and the dye pulses an electronic control system uses the intensity of the amplified pulses to feed back on the phase of the rf into the mode locker of the amplifying laser.

For the transient grating optical Kerr effect (TG-OKE) experiments described here, the amplified pulse is split into three pulses to yield the two excitation pulses and the probe pulse. The two excitation pulses, focused to 120 μm spot sizes, are crossed in the sample at an angle of 15° to produce an optical interference pattern (see Fig. 1). The optical interference pattern induces the OKE grating, which mimics the interference pattern spatially. This grating is monitored by the 90 μm spot size probe pulse which is incident at the phase matching angle for Bragg diffraction (slightly noncollinear with the excitation beam to achieve spatial separation). The probe pulse can be variably delayed by an optical delayline which is controlled by a 1 μm resolution stepper motor. The intensity as well as the polarization of all three beams can be independently controlled by sets of half-wave plates and linear polarizers. A fourth linear polarizer is set in the signal path and permits any polarization of the diffracted beam to be monitored. Typical single pulse energies used in the experiments were in the range 200 nJ–1 μJ. One of the excitation beams or the probe beam is chopped and the signal, which is picked up by a photodiode or a photomultiplier, is fed to a lock-in amplifier. The output of the lock-in amplifier is connected to a computer, which allows signal averaging by controlling multiple scans of the optical delayline.

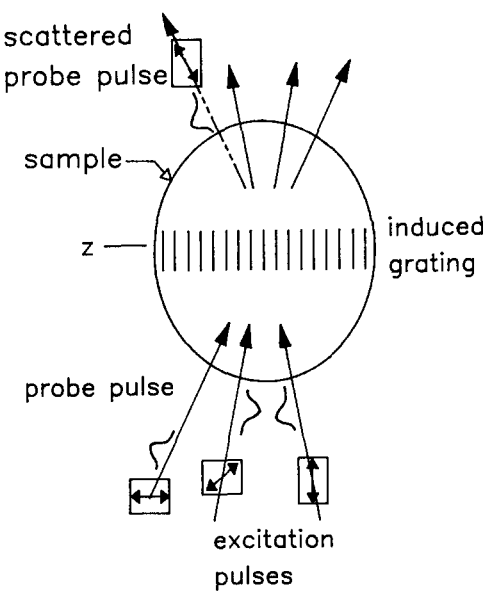

FIG. 1. Schematic illustration of the transient grating experiment. The crossed excitation pulses generate a periodic Kerr effect alignment in the sample with the wavelength of the optical interference pattern. The resulting changes in the index of refraction create a diffraction grating which Bragg scatters the probe pulse. The polarizations of all four pulses are controlled in the experiment and are used to separate electronic and nuclear Kerr effect in the detection.

Biphenyl (Fisher reagent grade) was extensively zone refined (≈300 passes) before use. *n*-heptane (Baker, for UV spectrophotometry) was used without further purification. The biphenyl liquid and biphenyl/*n*-heptane solutions were in a sealed 1 mm spectrophotometric cuvette. The sample under study was placed inside a sample holder whose temperature could be regulated and controlled within ± 0.2 °C. The viscosities of the biphenyl/*n*-heptane solutions were measured with a Cannon–Ubbelohde semimicro-type viscometer. The density over the investigated temperature ranges was calculated using the isobaric expansion formula. Literature values were used for the viscosity of neat biphenyl.[16] The biphenyl/*n*-heptane solutions investigated had weight ratios of 0.2:1 and 0.5:1 biphenyl:*n*-heptane corresponding to 0.77 mol/ℓ (at room temperature) and 1.65 mol/ℓ (at 50 °C). The high concentration sample had to be heated to ≈45 °C for all biphenyl to dissolve.

n-heptane has a small electronic polarization anisotropy of its own. However, TG-OKE experiments on a pure *n*-heptane sample showed that the contribution to the signal due to *n*-heptane molecules is negligible in the biphenyl/*n*-heptane samples.

III. THEORETICAL BACKGROUND

In a TG experiment the two time coincident laser excitation pulses which are crossed in the sample set up an optical interference pattern. If the length τ_p of the pulses is short compared to the characteristic response times of the sample this interference pattern generates a coherent spatially periodic response in the material which is given by the impulse response function $G(t)$ of the material. The probe pulse entering the sample at the Bragg angle is diffracted by this optical grating. If we can neglect absorption in the sample and only have to consider stimulated scattering phenomena (which is the case for the experiments described here), the intensity of the scattered light is

$$I(t) \propto |\chi^3(t)|^2 \propto |\delta\epsilon(t)|^2 \propto |G^{\epsilon\epsilon}(t)|^2. \quad (1)$$

Here $\chi^{(3)}$ is the third-order nonlinear susceptibility, ϵ is the dielectric constant, $\delta\epsilon$ is the peak–null difference of the dielectric constant in the optical grating, and $G^{\epsilon\epsilon}$ is the impulse response function of the dielectric constant of the sample. In a number of recent papers Nelson and co-workers have given a detailed description of the stimulated scattering grating experiment and have compared it to dynamic light scattering in the frequency domain.[17] The frequency resolved DLS spectrum is given by

$$I(\omega) \propto (kT/\omega)\mathrm{Im}[G^{\epsilon\epsilon}(\omega)], \quad (2)$$

with $G^{\epsilon\epsilon}(\omega)$ and $G^{\epsilon\epsilon}(t)$ being related by Fourier transform. So, in the limit of infinite time resolution and infinite frequency resolution, the TG and the DLS experiment contain the same information and monitor the same processes. Within the general framework of time correlation functions we can equally well describe the response of the system through

$$C^{\epsilon\epsilon}(t) = \langle \epsilon^*(0)\epsilon(t)\rangle, \tag{3}$$

the dielectric constant time correlation function. The relationship between $G^{\epsilon\epsilon}(t)$ and $C^{\epsilon\epsilon}(t)$ is simply given through time differentiation

$$G^{\epsilon\epsilon}(t) = -(1/kT)\left(\frac{\partial}{\partial t}\right)C^{\epsilon\epsilon}(t). \tag{4}$$

$\chi^{(3)}(t)$, $\delta\epsilon(t)$, $G^{\epsilon\epsilon}(t)$ and $C^{\epsilon\epsilon}(t)$ in Eqs. (1) and (4) are tensor quantities whose properties are determined through the symmetry group of the sample and the physical processes under investigation. We will only consider an isotropic sample, which is an appropriate description of a molecular liquid. There are three independent elements of $\chi^{(3)}$. Through the choice of the electric field polarizations of the two excitation beams, the probe beam and the signal beam, a certain projection of the tensor is selected, and a scalar quantity $I(t)$ is measured. Different choices for these polarizations allow us to evaluate different tensor elements of $\chi^{(3)}$ and $G^{\epsilon\epsilon}$ and single out different physical phenomena if these phenomena have different $\chi^{(3)}$ symmetry properties. For example, if all beams in the TG experiment are polarized perpendicular to the scattering plane (we will call this 0°) we measure $\chi^{(3)}_{1111}(t)$. In a polarization grating or crossed grating approach, one of the excitation beams is 0° polarized, the other has 90° polarization. If the probe beam is 0° polarized and we monitor the signal at 90° polarization, we determine $\chi^{(3)}_{1212}(t)$. In a more general case, the excitation beams have polarizations of 0° and α, the probe beam has 90° polarization and we detect the signal beam with a polarization angle β, then

$$I(t) \propto |\sin\beta\cos\alpha\,\chi^{(3)}_{1122}(t) + \sin\alpha\cos\beta\,\chi^{(3)}_{1212}(t)|^2. \tag{5}$$

So through the choice of α and β we can essentially monitor any combination of elements $\chi^{(3)}$. For example, it has been shown recently[18] that it is possible to distinguish between an excited state grating and a Kerr effect. This approach was pioneered by Etchepare *et al.*[19] In an elegant investigation of the Kerr effect in CS_2, they showed how to separate the nuclear and electronic contributions to the Kerr effect through polarization selective TG experiments. This separation is based on the different symmetry properties for the electronic $\chi^{(3)}_e$ and the nuclear $\chi^{(3)}_n$ processes.[20]

$$\chi^{(3)}_{e,1111} = 3\chi^{(3)}_{e,1212} = 3\chi^{(3)}_{e,1221} = 3\chi^{(3)}_{e,1122},$$
$$\chi^{(3)}_{n,1111} = (4/3)\chi^{(3)}_{n,1212} = (4/3)\chi^{(3)}_{n,1221} = -2\chi^{(3)}_{n,1122}. \tag{6}$$

As can be calculated from these relationships and Eq. (5), only nuclear contributions will be observed for $\alpha = 45°$ and $\beta = 135°$, and only electronic contributions will be observed for $\alpha = 45°$ and $\beta = 56.31°$. We have used these two configurations in our investigations to separate electronic and nuclear Kerr effect at early times $t < 2$ ps. We have used a pure polarization grating at longer times $t > 2$ ps, when the excitation pulses have left the sample and the instantaneous electronic effects have relaxed. The polarization grating gives, in general, a better S/N ratio as the polarizer in the signal beam screens out most of the background scattered light. It also suppresses contributions to the signal from optically generated acoustic waves which might play a role at times $t > 100$ ps.[12,21]

We are interested in the nuclear Kerr effect in molecular liquids. The excitation pulses interact with the polarizability of the sample and exert torques on the induced molecular dipole moments. One can distinguish between single molecule polarizability, which governs the response of individual molecules in the medium, and higher order polarizabilities, which determine the response of molecule pairs and oligomers.[22]

Molecular librations dominate the response of the sample at short times $t < 1$ ps. The interaction with the single molecule polarizability induces a reorientation of the molecules. It is the relaxation of this nonequilibrium orientational distribution by rotational motions of the molecules which we observe in our experiment for $t > 2$ ps. We will discuss the rotational motions and choose a specific model to describe them. The Debye diffusion model with hydrodynamic boundary conditions is capable of describing the phenomena for $t > 2$ ps. For shorter time, we will discuss the excitation and damping of the coherent librational motion which leads to the orientational anisotropy.

To explain our experimental results through molecular processes, we have to relate the observables in Eq. (1) to molecular quantities. In the data presented below there is no evidence for contributions from higher order polarizabilities, and, therefore, it is sufficient to consider the liquids as if they are composed of isolated molecules in dilute solution (we will consider the effect of correlation between particles later on). We can approximate the time correlation function of the dielectric constant ϵ by the time correlation function of the molecular polarizability α i.e.,

$$C^{\epsilon\epsilon}(t) \propto C^{\alpha\alpha}(t). \tag{7}$$

With Eq. (3), this gives

$$C^{\epsilon\epsilon}_{ij}(t) \propto \langle \alpha_{ij}(0)\alpha_{ij}(t)\rangle. \tag{8}$$

Here $C^{\epsilon\epsilon}_{ij}$ is the time correlation function for a certain selected projection of the dielectric tensor, as mentioned earlier, and α_{ij} is an element of the molecular polarizability tensor in a laboratory-fixed coordinate system. For every molecule there is a (molecular-fixed) principal axis system of the molecular polarizability in which only the diagonal elements α_{xx}, α_{yy}, and α_{zz} are nonzero. If the molecule has certain symmetry properties, this tensor can be simplified further, e.g., a cylindrically symmetric molecule has only two independent components $\alpha_\perp$ and $\alpha_\parallel$.[1]

For times greater than 2 ps, the OKE induced transient grating relaxes by orientational diffusion. The ultrafast time behavior is discussed in Sec. IV. An extremely successful model for the reorientation process was developed by Debye.[23] In this small-step diffusion model, molecules can only rotate by a small angle before they experience a reorienting collision. Under the assumptions of this model the complete reorientation process can be characterized by diffusion constants Θ_i. In the most general case there is a diffusion tensor with three independent diagonal elements Θ_{xx}, Θ_{yy}, and Θ_{zz} which characterize the reorientational motion around three independent axes. It can be shown that the reorientational relaxation process then is described by a sum of five exponentials.[24,25] To simplify matters, we introduce at this point two assumptions which are confirmed by the experimental

results. First, the principal axis systems for the polarizability tensor and the rotational diffusion tensor coincide or are very close to each other. This reduces the number of exponentials to be considered to two[24]:

$$C^{\epsilon\epsilon}(t) \propto A_1 \exp[-(6\Theta_I + 2\Delta)t] + A_2 \exp[-(6\Theta_I - 2\Delta)t], \quad (9a)$$

where

$$\Theta_I = (1/3)(\Theta_{xx} + \Theta_{yy} + \Theta_{zz}), \quad (9b)$$

$$\Delta = [(\Theta_{xx} - \Theta_{yy})^2 + (\Theta_{zz} - \Theta_{xx})(\Theta_{zz} - \Theta_{yy})]^{1/2}, \quad (9c)$$

$$A_1 = 1/N^2\{(a^2/3)[\alpha_{zz} - (1/2)(\alpha_{xx} + \alpha_{yy})]^2 + (ab/\sqrt{3})[\alpha_{zz} - (1/2)(\alpha_{xx} + \alpha_{yy})][\alpha_{xx} - \alpha_{yy}] + (b^2/2)[\alpha_{xx} - \alpha_{yy}]^2 \quad (9d)$$

with

$$a = \sqrt{3}(\Theta_{xx} - \Theta_{yy}), \quad (9e)$$

$$b = (2\Theta_{zz} - \Theta_{xx} - \Theta_{yy} + 2\Delta), \quad (9f)$$

$$N = 2(\Delta b)^{1/2}. \quad (9g)$$

A_2 is the same as A_1 with the exception that a and b are interchanged and a negative sign is placed in front of the ab term.

Second, the diffusion constants for the rotation around the two short axes of the biphenyl molecule (tumbling motion) are very similar

$$\Theta_{xx} \approx \Theta_{yy} \equiv \Theta_\perp, \quad (10a)$$

but different from the diffusion constant characterizing the rotation around the long axis (spinning motion)

$$\Theta_\perp \neq \Theta_\parallel \equiv \Theta_{zz}. \quad (10b)$$

Considering this second assumption of a symmetric diffusor we should bear in mind that the average dihedral angle between the two phenyl rings in biphenyl in the liquid phase is estimated to be 20°–40°.[26–30] Under these circumstances these assumptions appear to be physically well founded and consistent with the experiments presented below. Inserting Eqs. (10) into Eqs. (9) gives

$$C^{\epsilon\epsilon}(t) \propto A_1 \exp[-t/\tau_1] + A_2 \exp[-t/\tau_2] \quad (11a)$$

or

$$G^{\epsilon\epsilon}(t) \propto (A_1/\tau_1)\exp[-t/\tau_1] + (A_2/\tau_2)\exp[-t/\tau_2] \quad (11b)$$

with

$$\tau_1 = 1/6\Theta_\perp, \quad (11c)$$

$$\tau_2 = 1/(4\Theta_\parallel + 2\Theta_\perp), \quad (11d)$$

$$A_1 = (1/2)[\alpha_{xx} - \alpha_{yy}]^2, \quad (11e)$$

and

$$A_2 = (1/3)[\alpha_{zz} - (1/2)(\alpha_{xx} + \alpha_{yy})]^2. \quad (11f)$$

That is, we expect to see a sum of two exponential decays with their respective amplitude given by the anisotropy of the molecular polarizability and the decay times.

Hydrodynamic theories of liquids ignore the details of molecular interaction and treat the problem with a continuum theory. The only important parameters are the shear viscosity η of the medium and the boundary conditions at the surface of the molecules being probed.[31] The Stokes–Einstein–Debye (SED) equation,

$$\tau_r = 1/6\Theta = \eta V_m/kT \quad (12)$$

allows one to calculate the rotational relaxation time τ_r of a spherical particle under stick-boundary conditions.[1,31] Here V_m is the volume of the particle. Perrin extended this basic theory to treat cylindrically symmetric ellipsoids,[32] and Hu and Zwanzig showed how to calculate rotational relaxation times for these ellipsoids under slip-boundary conditions.[33] Their theories replace the molecular volume V_m in Eq. (12) by an effective volume,

$$V_{\text{eff}} = fzV_m, \quad (13)$$

with f being a shape factor and z depending on the hydrodynamic boundary conditions. The rotational relaxation of an ellipsoid with three different principal axes has been treated within this general framework by Youngren and Acrivos[34] allowing them to calculate three different effective volumes and relaxation times for any given ellipsoid.

Another extension of the basic SED equation was introduced by Alms *et al.*[35] who added a term τ_0

$$\tau_r = \eta V_{\text{eff}}/kT + \tau_0 \quad (14)$$

to account for the observed nonzero value of τ_r in the extrapolation $\eta/T \to 0$. τ_0 is generally associated with the unhindered inertial rotation of the molecule but has to be interpreted very carefully[31] as even negative values of τ_0 have been found experimentally.

The τ_r in Eqs. (12) and (14) are single particle correlation times. One can show, however, that the relaxation times measured in an TG-OKE experiment or a DLS experiment are collective relaxation times τ_c.[36] This is in contrast to, e.g., a NMR spin lattice relaxation or fluorescence depolarization experiment which measure single particle correlation times. Keyes and Kivelson[37] have given an approximate theory for the relation between τ_r and τ_c and find

$$\tau_c = (g_2/j_2)\tau_r. \quad (15)$$

g_2 and j_2 are static and dynamic orientation correlation parameters and it is usually assumed that $j_2 \approx 1$.[1] Therefore, a separate measurement of τ_c and τ_r through different experimental approaches or a measurement of the relaxation times in dilute solution and neat liquid yields g_2 and information about orientational order in the liquid sample. From Eqs. (14) and (15) we expect the correlation times τ_c measured in a TG-OKE experiment to be given by

$$\tau_c = g_2(\eta V_{\text{eff}}/kT + \tau_0). \quad (16)$$

IV. RESULTS AND DISCUSSION

Figure 2 shows typical TG-OKE signals as observed in experiments under different polarization configurations. To display the fast time scale behavior [Fig. 2(a)] the nuclear-only OKE (0°/45°/90°/135°) and the electronic-only OKE (0°/45°/90°/56.31°) configurations were chosen (the angles of polarization in the preceding parentheses stand for the two excitation beams, the probe beam and the signal beam in that sequence). The electronic-only OKE signal [trace 1 in Fig. 2(a)] gives the instrument response of the experiment

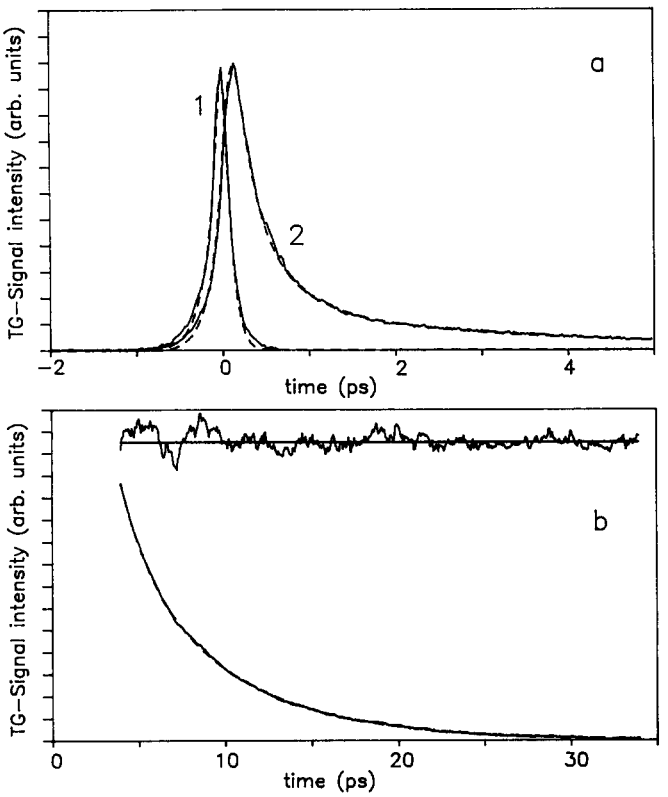

FIG. 2. Optical Kerr effect transient grating signals $S(t)$ for a 0.77 mol/ℓ biphenyl/*n*-heptane solution at 23 °C. (a) Fast time scale behavior. Signals 1 and 2 are recorded with the electronic-only (0°/45°/90°/56°) and nuclear-only (0°/45°/90°/135°) TG-OKE polarization configuration, respectively. The dashed lines through the signals are calculated through the evaluation of convolution integral (17). The theoretical curve through signal 2 (the nuclear Kerr response) is calculated with response function (20). Signal 1 (the electronic Kerr or instrument response) has been fit with a $\delta(t)$ sample response function. (b) Slow time scale behavior of the signal, recorded with the polarization grating configuration (0°/90°/0°/90°). The dashed line is a fit using a biexponential decay function. The upper trace shows the residuals of the fit on a 10× enlarged vertical scale.

as the relaxation time of the electronic OKE is fast (10^{-15} s) compared to the pulsewidth. We have fit the instrument response by assuming a double-sided exponential shape $I(t)$ for the laser pulse[14] with $1/e$ widths of 45 and 145 fs and calculating the TG convolution integral for the three pulses with a δ function for the sample response $G^{\epsilon\epsilon}(t)$

$$S(t) = \int_{-\infty}^{+\infty} I_p(t-t'') \times \left[\int_{-\infty}^{t''} G^{\epsilon\epsilon}(t''-t')I_e(t')dt'\right]^2 dt''. \quad (17)$$

$I_e(t)$ and $I_p(t)$ are the excitation and probe pulse shapes (identical in our case), $S(t)$ is the signal amplitude of the diffracted light when the probe pulse arrives with a delay t with respect to the excitation pulses. The dashed line, which is the fit to curve 1 in Fig. 2(a), shows that the assumed pulse shape reproduces the measured instrument response very well. Only in the far wings are there small deviations from the analytical function used.

Trace 2 in Fig. 2(a) and the curve in Fig. 2(b) display the nuclear OKE data. First, we will address times >2 ps where the dynamics are determined by reorientational diffusion. As seen in Fig. 2(a), the TG signal due to the nuclear OKE data vanishes at a set of angles appropriate for the $\chi^{(3)}$ tensor symmetry associated with single particle polarizability. This validates the assumption that the dynamics can be described in terms of single particle reorientation. The reorientational relaxations have characteristic decay times much longer than the pulsewidth. Therefore, one can analyze the $t>2$ ps data in a straightforward manner without having to numerically compute convolution integrals. Convolution will be used in discussing the $t<2$ ps data.

We have used the following approach in analyzing the data. A TG experiment measures a signal which is proportional to the square of the response function $G^{\epsilon\epsilon}(t)$. Thus, we first calculate $\sqrt{S(t)}$ for the observed signal and then work with this function. Figure 3(a) shows a semilogarithmic plot of the $\sqrt{S}$ data in Fig. 2(b). The decay of the signal for $t \geqslant 12$ ps is described by an exponential decay with a time constant $\tau_1 = 12.3$ ps. At shorter times, $t<12$ ps, the signal deviates from a single exponential. To analyze this part of the signal, we have subtracted the contribution of the slow exponential $B_1 \exp[-t/\tau_1]$ from $\sqrt{S(t)}$ and drawn a semilogarithmic plot of the difference. This plot for the $\sqrt{S}$ data in Fig. 2(a) is shown in Fig. 3(b). We find a straight line over three factors of e characterizing another exponential with a time constant $\tau_2 = 2.1$ ps (and amplitude B_2). So, for $t \geqslant 2$ ps the signal decay $\sqrt{S(t)} \propto G^{\epsilon\epsilon}(t)$ is given by a biexponential function $B_1 \exp[-t/\tau_1] + B_2 \exp[t/\tau_2]$. The dashed line through the data in Fig. 2(b), barely discernable from the data, is the square of this biexponential function and demonstrates the excellence of the fit. In the upper part of Fig. 2(b), the residuals of the fit are shown on a 10 times expanded scale. There is no systematic trend in the residuals which supports the accuracy of the fit. The ultrafast time scale behavior ($t<2$ ps) shows additional contributions to the signal which are discussed later.

The general behavior described in connection with Figs. 2 and 3 is shared by all samples over the entire temperature range investigated. For $t \geqslant 2$ ps, the decay of $G^{\epsilon\epsilon}(t)$ is given by a biexponential characterized by two time constants τ_1 and τ_2. Table I shows a compilation of the decay parameters found in the experiments. The decay times are the average of several independent measurements. From the theoretical background presented earlier we now identify the decay function with Eq. (11b) and associate the two decay parameters $\tau_1 = 1/6\Theta_\perp$ and $\tau_2 = 1/(4\Theta_\parallel + 2\Theta_\perp)$ with rotational diffusion constants. τ_1 characterizes the slower tumbling around the short axes whereas τ_2 contains contributions from spinning and tumbling motion. From Eqs. (11c) and (11d), we can calculate the time constant for pure spinning motion

$$\tau_x = 1/6\Theta_\parallel = \frac{2\tau_1\tau_2}{3\tau_1 - \tau_2}. \quad (18)$$

The values of τ_x are also compiled in Table I.

We have plotted the values of τ_1 and τ_x vs η/T in Figs. 4 and 5, respectively. Focusing first on the behavior of the slowest exponential, depicted in Fig. 4, we find that τ_1 shows a linear dependence on η/T, as predicted by the modified SED equation (16). The straight line in Fig. 4 is a linear fit

TABLE I. Average rotational correlation times of the investigated samples. τ_1 and τ_2 are the measured relaxation times of the biexponential decay. τ_x is the relaxation time characterizing the spinning motion of the molecule and is calculated according to Eq. (18) in the text. T is the temperature in °C and η is the viscosity in centipoise (cP). The data points marked with an asterisk are taken in the supercooled biphenyl liquid.

	T (°C)	η (cP)	η/T (10^{-3} cP/K)	τ_1 (ps)	τ_2 (ps)	τ_x (ps)
Biphenyl, neat						
	58*	1.93	5.82	38.5	5.7	4.0
	63*	1.75	5.21	34.9	5.3	3.7
	73	1.46	4.21	28.3	4.3	3.0
	83	1.23	3.44	24.8	3.0	2.1
	103	0.89	2.37	17.7	2.9	2.0
	113	0.77	2.00	15.3	2.4	1.7
	124	0.67	1.68	13.6	2.4	1.7
Solution 1.65 mol/ℓ						
	49	0.43	1.35	12.3	2.3	1.6
	56	0.41	1.24	11.2	2.2	1.6
	63	0.38	1.14	10.6	2.1	1.5
	78	0.34	0.96	8.8	2.0	1.5
Solution 0.77 mol/ℓ						
	23	0.48	1.61	12.1	2.1	1.4
	35	0.42	1.38	10.5	2.0	1.4
	49	0.38	1.19	9.1	1.9	1.4
	63	0.35	1.04	7.7	1.7	1.2
	78	0.32	0.91	6.8	1.6	1.2

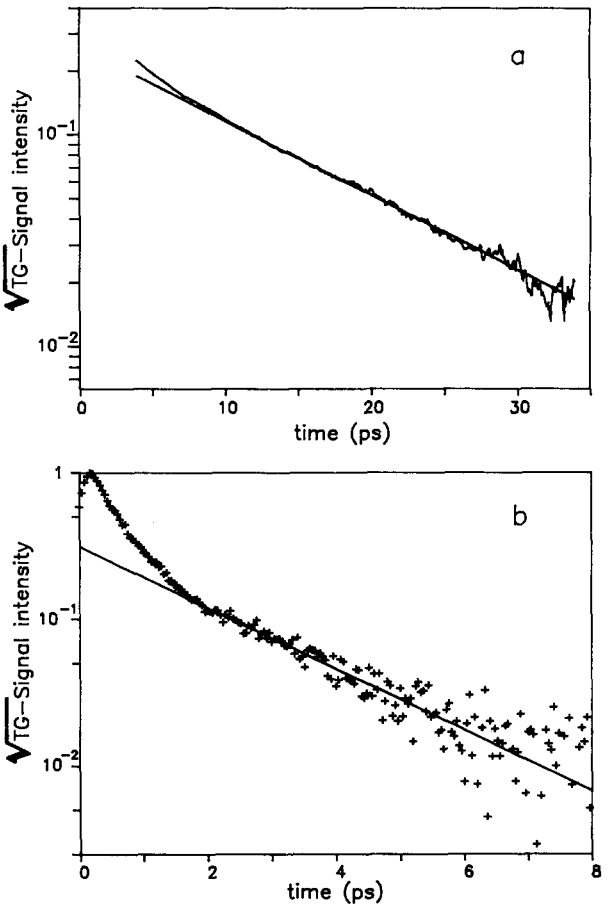

FIG. 3. Analysis of the data in Fig. 2. (a) Semilogarithmic plot of $\sqrt{S(t)}$ in Fig. 2(b). The straight line is a monoexponetial fit to the slow time scale tail of the decay. (b) Semilogarithmic plot of $\sqrt{S(t)}$ [signal 2 in Fig. 2(a)] after subtraction of the slow time scale exponential decay $B_1 \exp[-t/\tau_1]$ as shown in (a). The straight line is a single exponential fit to the $t > 2$ ps part of the curve following subtraction.

for the relaxation times observed in neat biphenyl and is given by $\tau_1 = (3.4 \pm 1.0) \times 10^{-12}$ s $+ (6.0 \pm 0.2) \times 10^{-9}$ (η/T) s K/cP. The first number is the intercept, and the second is the slope. Applying Eq. (16) this slope corresponds to $g_2 V_{\text{eff}} = 83 \pm 3$ Å^3. Similar linear fits for the data in solution (fits not shown in Fig. 4) give $\tau_1 = (0.0 \pm 0.7) \times 10^{-12}$ s $+ (9.1 \pm 1.8) \times 10^{-9}$ (η/T) s K/cP for the 1.65 mol/ℓ solution and $\tau_1 = (0.0 \pm 1.0)$ 10^{-12} s $+ (7.6 \pm 0.9)$ 10^{-9} (η/T) s K/cP for the 0.77 mol/ℓ solution. This corresponds to $g_2 V_{\text{eff}} = 126 \pm 25$ Å^3 and 105 ± 12 Å^3 for the 1.65 mol/ℓ sample and the 0.77 mol/ℓ sample, respectively. That is, the solution data show somewhat larger slopes and have larger error margins. The larger error margins can be attributed to two facts. First, the S/N ratio for the data in solution is worse than for the signals in neat biphenyl, as the signal intensity decreases with the number of biphenyl molecules in the sample. Second, the η/T range which is easily accessible and has been investigated for the solutions is much narrower than the η/T range of the neat biphenyl data. This is because of the larger activation energy of the viscosity in neat biphenyl compared to the solutions and the fact that it is possible to supercool the neat biphenyl considerably ($\approx 15°$) (see data points at 58 and 63 °C) and extend the accessible temperature and viscosity range.

If there is any orientational correlation between the biphenyl molecules, we would expect that this correlation, contained in the parameter $g_2 V_{\text{eff}}$, would increase with increasing biphenyl concentration and increasing interaction between the molecules. This is clearly not the case. $g_2 V_{\text{eff}}$ is smaller in the neat biphenyl than in the two solutions, and the error bars almost overlap. Although it might be possible to construct a complex model, including specific interac-

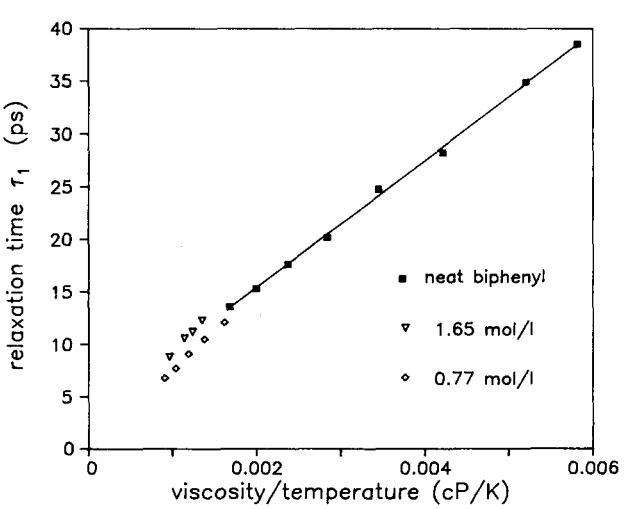

FIG. 4. η/T dependence of decay time τ_1 of slow exponential decay. The straight line is a linear fit through the data for neat biphenyl only.

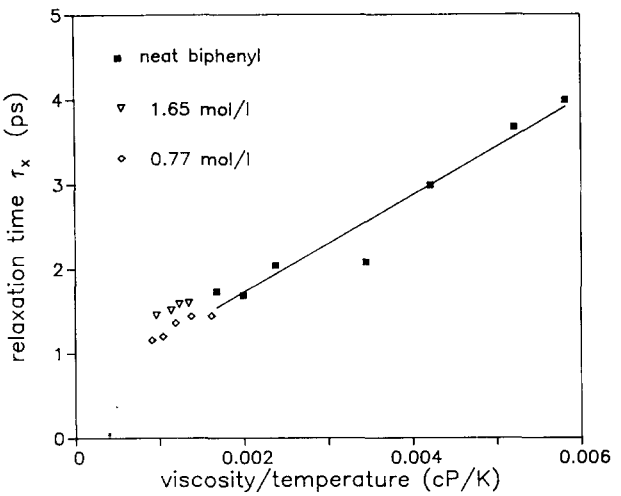

FIG. 5. η/T dependence of "fast" correlation time τ_x as calculated with Eq. (18). The straight line is a linear fit through the data for neat biphenyl only.

tions with the *n*-heptane solvent molecules, which would account for an increase in g_2 going from the 0.77 mol/ℓ to the 1.65 mol/ℓ solution and then a drop of the orientational correlation or even an anticorrelation in the neat liquid, the available data, especially given the large error margins for the solution experiments, supports a simple conclusion. The fact that there is no obvious trend going from the least concentrated solution to the neat liquid indicates that there is little orientational correlation between the biphenyl molecules, and $g_2 \approx 1$.

This conclusion is supported by a comparison with calculated numbers. We determined the molecular extensions of biphenyl using a Stuart–Briegleb space filling model and approximated the molecule as a cylindrically symmetric ellipsoid whose large diameter is given by the long axis of the biphenyl molecule and whose short diameter is the mean of the two short axes of biphenyl. This gives a molecular volume $V_m = 122$ Å^3, and an asphericity parameter, $\rho = 0.42$. Assuming slip-boundary conditions,[1,31] we find[33] $V_{\text{eff}} = 104$ Å^3, a value of the same magnitude as the experimental values found for $g_2 V_{\text{eff}}$. This supports the conclusion that the orientational correlation between the biphenyl molecules is small and that $g_2 \approx 1$ in the samples investigated. Altogether, the data show that the tumbling motion reorientational relaxation of biphenyl is well described by hydrodynamic theory.

Turning to the τ_x data in Fig. 5 we again find a linear dependence of τ_x on η/T as predicted by the SED equation. The results of linear fits through the data are $\tau_x = (0.6 \pm 0.3) \times 10^{-12}$ s $+ (5.7 \pm 0.5) \times 10^{-10}$ (η/T) s K/cP for the neat biphenyl (shown as straight line in Fig. 5), $\tau_x = (1.1 \pm 0.1) \times 10^{-12}$ s $+ (4.1 \pm 2.8) \times 10^{-10}$ (η/T) s K/cP for the 1.65 mol/ℓ solution, and $\tau_x = (0.8 \pm 0.1) \times 10^{-12}$ s $+ (4.1 \pm 1.4) \times 10^{-10}$ (η/T) s K/cP for the 0.77 mol/ℓ solution. Within the experimental error, these slopes are the same. This indicates that the fast reorientational relaxation given by τ_x is well described by hydrodynamic theory. The comparable slope for the neat biphenyl and solution data demonstrates that there is no appreciable static orientational correlation for the short axes of biphenyl and g_2 (short axes) ≈ 1.

Since $g_2 \approx 1$, the slopes for τ_x vs η/T can be translated into an effective hydrodynamic volumes V_{eff} of 7 Å^3. If biphenyl is approximated as a general ellipsoid with three different diameters, three effective hydrodynamic volumes for slip boundary conditions can be calculated.[34] One value calculated in this manner is $V_{\text{eff}} = 8$ Å^3. It is, however, unrealistic to approximate the biphenyl molecule with its two out-of-plane phenyl rings as a general ellipsoid. There is no unambigous way to do it.

Instead, it is informative to compare the spinning motion of biphenyl with the rotation of benzene around an in-plane axis. Alms *et al.*[38] have found from the viscosity dependence of τ_1 of benzene that $\tau_1 = 3.5 \times 10^{-12}$ (η)s/cP. This correponds to $V_{\text{eff}} = 14.3$ Å^3, compared to the theoretical value for slip-boundary conditions, $V_{\text{eff}} = 20.4$ Å^3. That is, the τ_x for rotation of biphenyl around its long axis are smaller than the reorientation times of benzene. The fact that the biphenyl molecule spins faster than benzene at the same viscosity contradicts our intuition about the reorientational relaxation of these molecules. We have considered two possible reasons for the surprisingly fast relaxation of biphenyl.

First, the spinning motion of biphenyl might have to be described with subslip-boundary conditions. Subslip-boundary conditions are generally explained by picturing a small nonspherical molecule rotating in a solvent of large molecules with large interstitial gaps providing little friction.[31,39] Although a solution of biphenyl in *n*-heptane or neat biphenyl liquid do not seem to fit into this category, we cannot totally exclude this possibility.

Second, the fast reorientational relaxation might not be associated with spinning of the rigid biphenyl molecule but result from a torsional motion of the two phenyl rings with respect to each other around the central C–C bond. If the molecule is not rigid, the optical excitation pulses not only exert a torque on the whole molecule, but also exert different torques on the two phenyl rings. This induces a torsion of the molecule and a change of the dihedral angle between the two phenyl rings. The twisted molecule relaxes by intramolecular reorientation of the phenyl rings. The internal relaxation takes place within a restricted range of the dihedral angle determined by the potential function describing the internal rotation in the presence of the liquid environment. It has been shown that molecular reorientational diffusion, which can only proceed within a limited angular region, is characterized by an apparently faster relaxation time than reorientation without restriction.[40,41]

A recent determination of the biphenyl dihedral angle potential function[26] gives barrier heights of 4.7 and 14.7 kJ/mol at 0° and 90°. Hence, even at room temperature, there is a considerable probability (≈ 0.15) of crossing the barrier at 0°. Experiments at higher temperature than presented here might be able to clarify the nature of this fast reorientational diffusion process, since reorientation of the whole molecule and internal rotation in a potential well should show a different T dependence. The conditions in the liquids studied here are not those which would be expected to yield

subslip-boundary conditions. Internal dihedral angle relaxation seems the most likely explanation for the faster relaxation component.

It is interesting to compare the results of the time domain TG-OKE experiments with the results of a frequency domain DLS study. Dorfmüller[13] has published data from a DLS investigation of several biphenyl/*n*-heptane solutions, one having a concentration of 0.77 mol/ℓ, allowing direct comparison with our data. The scattered Rayleigh spectrum was fit with a single Lorentzian which was associated with the tumbling motion of the biphenyl molecule. Besides some discrepancy at low temperature/high viscosity, the linewidth of this Lorentzian is consistent with the time constant of the slow exponential in the TG-OKE experiments. The important difference between the DLS and the OKE data is that the time resolved experiments show a distinct second relaxation component. The fast component (and the ultrafast relaxation discussed below) are not observed in the frequency domain study, although theoretically both methods should reveal the same information.

The different observations in the TG-OKE and DLS experiments could be due to different experimental constraints in the two approaches. First, the light scattering method has the largest signal and best S/N ratio for small values of $\Delta\omega$ characterizing the slow processes in the sample. Signal and S/N ratio get smaller in the spectral wings, which contain information on the fast dynamics. In a time resolved experiment, however, the fast processes dominate the signal at early times where the intensity of the signal is large and the S/N ratio high. Only the contributions of the slow relaxation processes are left at long times where the signal intensity and S/N ratio are small. Second, the time resolved method, given a long enough optical delay line, is able to gather data on all time scales with a single experimental setup. Depending on the free spectral range of the equipment used, frequency resolved studies often involve different setups for different frequency scales. This can introduce problems with matching of the spectra and finding the correct baseline.

Dorfmüller[13] has also presented a linewidth analysis of Raman spectra of the symmetric breathing vibration of the phenyl ring of biphenyl in a 1.45 mol/ℓ biphenyl/CCl_4 solution. He finds correlation times, $\tau_{\text{ram}} = 4.5$–7.5 ps, which he associates with the spinning motion of biphenyl. These correlation times τ_{ram} are considerably longer than the relaxation times τ_x of the fast exponential found in the OKE experiments. As shown by Bartoli and Litovitz,[42] however, the reorientational correlation function for a Raman active vibration in a molecule of lower symmetry than C_{3v} or D_{3d} is a sum of five terms with different decay constants. It is not possible to isolate one of these terms and study reorientational motion about one specific axis of the molecule. Therefore, the values for τ_{ram} of biphenyl in Ref. 13 should contain contributions from the tumbling motion, making τ_{ram} longer than the values for τ_x found in the OKE study.

Up to now we have only considered the decay times τ_1 and τ_2 of the two reorientational relaxation components encountered in the TG-OKE experiment. Besides the decay constants, the two exponentials are also characterized by amplitudes B_1 and B_2. Following the theory leading to Eqs. (11), these should be given by the ratio of the anisotropies of the polarizability and the decay times, i.e., $B_i = A_i/\tau_i$. The values of B_1/B_2 found in the TG-OKE experiments are in the range 1.1–1.4. The independent values of the biphenyl polarizabilities, α_{ii},[43–45] which would allow us to calculate A_1/A_2, all have considerable shortcomings and are not consistent with one another. The values of α_{ii} found in the only experimental study[43] are based on the assumption of a flat biphenyl molecule and yield $A_1/A_2 = 0.96$. Two different theoretical treatments give $A_1/A_2 = 0.83$–0.94[44] and 3.7–4.8[45] for a dihedral angle of 30°–40°. Both theoretical approaches have critical flaws. The CNDO/SCI method[44] is based on a very deficient one-particle basis set, and the ACF method[45] is a purely empirical and conceptually weak approach.[46] The values of α_{ii} in Refs. 43 and 44 translate into $B_1/B_2 = 0.14$–0.20, whereas Ref. 45 gives $B_1/B_2 = 0.55$–1.05 compared to our experimental value of 1.1–1.4.

The difference between the calculated and experimental value of B_1/B_2 could arise from our imprecise knowledge of the α_{ii}. There is, however, a fundamental flaw in the description of the reorientational relaxation through Eqs. (11), i.e., the assumption of a purely relaxational mode. To see the limits of this picture, we will briefly discuss the dynamics on the ultrafast time scale $t < 2$ ps. Recent measurements on other systems[7–11] have reached the conclusion that the ultrafast timescale is dominated by the dynamics of librational modes. The excitation pulses exert a torque on the molecule and kick it out of its equilibrium orientation. The original motion is inertial and the molecule starts to librate within the potential well defined by its solvent cage. This can be thought of quantum mechanically as stimulated rotational Raman excitation of the libration. The librations are damped through collisions with other molecules. Whether the librations are underdamped or overdamped depends on specific molecular interactions.[9] In spite of this broad picture, the detailed description remains fuzzy. Up to now the available data are scarce. With one exception,[9] all investigations have been done at a single temperature, and it is difficult to decide between the response functions which have been put forward to describe the ultrafast dynamics.

With this background, we want to bring forward a major point which has been neglected so far; coherent librational motion and incoherent diffusive reorientational motion in a liquid are coupled. The molecule kicked by the electric field (Raman scattered) starts librating within the potential defined by its environment. In a crystal, the molecular libration damps by phonon scattering, and the molecule relaxes to its initial equilibrium orientation. In a crystal, after librational relaxation, there is no residual anisotropy. In a liquid, the libration is damped by collisions with neighboring molecules. At the same time, the solvent cage around the molecule is undergoing structural relaxation. Partial relaxation of the solvent structure is responsible for the net alignment (anisotropy) left in the sample after the damping of the libration. The librations are excited in preferred directions. Most of the induced alignment disappears with the librational damping. When the excited molecules damp, the local structure has changed. The molecules do not relax to their original configurations. It is only this residual align-

ment which relaxes by diffusive reorientational relaxation.

This picture has certain implications. If the time scale for the evolution of the solvent cage is much slower than the time scale for the librational damping, then the residual alignment following librational damping is very small. An extreme case would be the situation in the crystal mentioned above. The closer the damping and structural relaxation time scales are to each other, the larger is the alignment which then relaxes due to reorientational motion. The data shown in Figs. 2 and 3 are dominated by the librational contribution on the ultrafast time scale and can only be fit by assuming an inertial delay in the response function. This proves that the model of a purely relaxational mode is not applicable and the response function (11b) has to be modified at early tines. It also means that the expressions for the amplitudes of the exponentials in Eq. (11b) are incorrect and the discrepancy between the experimental values of B_1/B_2 and the values derived from Eq. (11b) are not surprising.

A correct response function has to describe the librational excitation and damping, the diffusive reorientational motion, *and* the coupling between the two kinds of motion. To take these into account, we have used a response function for a single libration/reorientation of the form

$$G^{ee}(t) = C_l[\exp(-t/\tau_b) - \exp(-t/\tau_a)] + C_r[1-\exp(-t/\tau_b)]\exp(-t/\tau). \quad (19)$$

The C_l term describes the libration as an overdamped oscillator characterized by time constants τ_a and τ_b. τ_a characterizes the rise of the libration induced anisotropy, and τ_b characterizes the decay of the libration. The C_r term describes the diffusive reorientation; the $[1-\exp(-t/\tau_b)]$ factor assures the coupling between librational and reorientational relaxation and delays the onset of the diffusive reorientation by the librational damping time. τ is the orientational diffusive relaxation time. Although earlier publications have acknowledged the fact that the reorientational relaxation should show inertial character at short times,[9,47] to our knowledge this is the first effort to explicitly link the librational and the diffusive reorientational motion.

One immediate implication of the picture of molecular dynamics developed here is the fact that C_l and C_r in Eq. (19) are not independent parameters but are related. C_r/C_l depends on the relationship between the time scales for the librational damping and the solvent structure evolution. If we associate the time scale for the solvent structure randomization with the time constants of the reorientational relaxation τ_i (this does not imply that they are identical), then C_r/C_l should be a function of t_b/τ_i, the ratio of the librational damping time and the reorientational relaxation time. If the librational damping does not depend strongly on temperature/viscosity, then we expect C_r/C_l to increase with increasing temperature/decreasing viscosity, i.e., decreasing τ_i. A check of the data, comparing the intensity of the signal at its maximum (when it is dominated by the libration) with the intensity at $t = 3$ ps (when the diffusive reorientation is predominant), actually shows a trend confirming this idea.

Equation (19) is in some respects heuristic. Its purpose is to explicitly link the librational motion and the reorientational relaxation. The librational motion might be more accurately described with an underdamped oscillation and a decay dominated by inhomogeneous dephasing, as in the recent publications of the groups of Nelson and Kenney-Wallace. However, thermalization (librational damping) must occur before the system can undergo diffusive relaxation. The coupling term between the librational and reorientational relaxation may also require a more refined treatment. Nevertheless, Eq. (19) contains the essential ingredients of a proper description of the dynamics.

To calculate the data on the ultrafast timescale $t < 2$ ps, we convolve the response function with the laser pulses following Eq. (17). To achieve a satisfying agreement between the data and the theoretical curve we include two ultrafast components in the response function, one for each of the two long time ($t > 2$ ps) decays. We have given this additional component the form of another overdamped oscillator. The two librations, like the two diffusive reorientational components, could correspond to motions around the long axis and the short axes of the biphenyl molecule. The resulting equation is

$$G^{ee}(t) = C_{l,1}[\exp(-t/\tau_{b,1}) - \exp(-t/\tau_a)] + C_{r,1}[1-\exp(-t/\tau_{b,1})]\exp(-t/\tau_1) + C_{l,2}[\exp(-t/\tau_{b,2}) - \exp(-t/\tau_a)] + C_{r,2}[1-\exp(-t/\tau_{b,2})]\exp(-t/\tau_2). \quad (20)$$

The calculated curve (dashed line) through the data in trace 2 of Fig. 2(a) uses the parameters: $C_{l,1} = 90$, $C_{l,2} = 3.4$, $\tau_a = 40$ fs, $\tau_{b,1} = 50$ fs, $\tau_{b,2} = 480$ fs, $C_{r,1} = 1$, $C_{r,2} = 1.12$, $\tau_1 = 2.1$ ps, and $\tau_2 = 12.3$ ps. The agreement is very good, but due to the limited time resolution of our experiments the first five parameters characterizing the ultrafast dynamics have an error margin of $\pm 20\%$. It is important to mention again that the data cannot be fit with a relaxational model, even using a number of additional exponentials. The data clearly display a delayed rising edge, consistent with the proposed description and response function.

V. CONCLUDING REMARKS

We have employed time resolved TG-OKE experiments in the study of the reorientational dynamics of biphenyl in liquids. The sub-ps time resolved investigation of biphenyl as neat biphenyl and in *n*-heptane solution reveals a biexponential decay ($t > 2$ ps) associated with the anisotropic reorientational relaxation of the molecule. The slower exponential is due to the tumbling motion of biphenyl and has been found in earlier DLS experiments. The faster exponential characterizes relaxation most likely arising from internal reorientational motion of the two phenyl rings around the central C–C bond. This faster component has not been seen in the DLS investigations. On the ultrafast time scale ($t < 2$ ps), dynamics are dominated by librational excitation and damping, rather than diffusive reorientational motion. Our experimental results demonstrate the limits of a purely relaxational model in describing the onset of molecular alignment. We have outlined an improved model which couples the diffusive reorientational relaxation of the molecules with the librational motion on the ultrafast time scale.

ACKNOWLEDGMENTS

This work was supported by the National Science Foundation, Division of Material Research (DMR 87-18959). Additional support was provided by the Office of Naval Research, Physics Division (N00014-85-K-0409). F.W. Deeg would like to thank the scientific commitee of NATO for a postdoctoral fellowship administered through DAAD.

[1]B. J. Berne and R. Pecora, *Dynamic Light Scattering* (Wiley, New York, 1976).
[2]*Molecular Liquids—Dynamics and Interactions*, edited by A. J. Barnes, W. J. Orville-Thomas, and J. Yarwood (Reidel, Dordrecht, 1984).
[3]W. G. Rothschild, *Dynamics of Molecular Liquids* (Wiley, New York, 1984).
[4]G. R. Fleming, *Chemical Applications of Ultrafast Spectroscopy* (Oxford University, New York, 1986), Chap. 6; R. M. Hochstrasser, Hyperfine Interact. **38**, 635 (1987).
[5]J. Etchepare, G. Grillon, R. Muller, and A. Orszag, Opt. Commun. **34**, 269 (1980).
[6]B. I. Greene and R. C. Farrow, Chem. Phys. Lett. **98**, 273 (1983).
[7]S. Ruhman, L. R. Williams, A. G. Joly, B. Kohler, and K. A. Nelson, J. Phys. Chem. **91**, 2237 (1987).
[8]S. Ruhman, B. Kohler, A. G. Joly, and K. A. Nelson, Chem. Phys. Lett. **16**, 141 (1987).
[9]S. Ruhman, L. R. Williams, A. G. Joly, and K. A. Nelson, IEEE J. Quantum Electron. **24**, 470 (1988).
[10]C. Kalpouzos, W. T. Lotshaw, D. McMorrow, and G. A. Kenney-Wallace, J. Phys. Chem. **91**, 2028 (1987).
[11]W. T. Lotshaw, D. McMorrow, C. Kalpouzos, and G. A. Kenney-Wallace, J. Chem. Phys. Lett. **136**, 323 (1987).
[12]G. Eyring and M. D. Fayer, J. Chem. Phys. **81**, 4314 (1984).
[13]Th. Dorfmüller, in *Rotational Dynamics of Small and Macromolecules*, edited by Th. Dorfmüller and R. Pecora (Springer, Berlin, 1987).
[14]V. J. Newell, F. W. Deeg, S. R. Greenfield, and M. D. Fayer, J. Opt. Soc. Am. **2** (in press).
[15]F. W. Deeg and M. D. Fayer (in preparation); F. W. Deeg, V. J. Newell, S. R. Greenfield, J. J. Stankus, and M. D. Fayer (in preparation).
[16]H. A. Kierstead and J. Turkevich, J. Chem. Phys. **12**, 24 (1944).
[17]Y. X. Yan, L. F. Cheng, and K. A. Nelson, Adv. Infrared Raman Spectrosc. **16**, 299 (1987); Y. X. Yan and K. A. Nelson, J. Chem. Phys. **87**, 6240, 6257 (1987).
[18]F. W. Deeg and M. D. Fayer, J. Chem. Phys (to be submitted).
[19]J. Etchepare, G. Grillon, J. P. Chambaret, G. Harmoniaux, and A. Orszag, Opt. Commun. **63**, 329 (1987).
[20]R. W. Hellwarth, Prog. Quantum Electron. **5**, 1 (1977).
[21]M. D. Fayer, IEEE J. Quantum Electron **22**, 1437 (1986).
[22]D. Kivelson and P. A. Madden, Annu. Rev. Phys. Chem. **31**, 523 (1980).
[23]P. Debye, *Polar Molecules* (Dover, New York, 1929).
[24]Reference 1, Chap. 7.
[25]L. D. Favro, Phys. Rev. **119**, 53 (1960).
[26]M. Akiyama, T. Watanabe, and M. Kakihana, J. Phys. Chem. **90**, 1752 (1986).
[27]A. d'Annibale, L. Lunazzi, A.C. Boicelli, and D. Maciantelli, J. Chem. Soc. Perkin Trans. 2 **1973**, 1396.
[28]V. J. Eaton and D. Steele, J. Chem. Soc. Faraday Trans. 2 **69**, 1601 (1973).
[29]E. D. Schmid and B. Brosa, J. Chem. Phys. **56**, 6267 (1972).
[30]H. Suzuki, Chem. Soc. Jpn. **32**, 1340 (1959).
[31]D. Kivelson, in *Rotational Dynamics of Small and Macromolecules*, edited by Th. Dorfmüller and R. Pecora (Springer, Berlin, 1987).
[32]F. Perrin, J. Phys. Radium **5**, 497 (1934).
[33]C. Hu and R. Zwanzig, J. Chem. Phys. **60**, 4354 (1974).
[34]G. K. Younggren and A. Acrivos, J. Chem. Phys. **63**, 3846 (1975).
[35]G. Alms, D. Bauer, J. Brauman, and R. Pecora, J. Chem. Phys. **59**, 5310, 5321 (1973).
[36]Reference 1, Chap. 12.
[37]T. Keyes and D. Kivelson, J. Chem. Phys. **56**, 1057 (1972).
[38]G. R. Alms, D. R. Bauer, J. I. Brauman, and R. Pecora, J. Chem. Phys. **58**, 5570 (1973).
[39]J. Dote and D. Kivelson, J. Phys. Chem. **87**, 3889 (1983).
[40]C. C. Wang and R. Pecora, J. Chem. Phys. **72**, 5333 (1980).
[41]M. P. Warchol and W. E. Vaughan, Adv. Mol. Relaxation Interaction Processes **13**, 317 (1978).
[42]F. J. Bartoli and T. A. Litovitz, J. Chem. Phys. **56**, 413 (1972).
[43]R. J. W. Le Fevre and D. S. N. Murthy, Aust. J. Chem. Soc. **21**, 1903 (1968).
[44]D. Bhaumik, H. H. Jaffe, and J. E. Mark, J. Mol. Struct. **87**, 81 (1982).
[45]J. D. McKinney, K. E. Gottschalk, and L. Pedersen, J. Mol. Struct. **105**, 427 (1983).
[46]W. Allen (private communication).